Supplement of Atmos. Chem. Phys., 21, 8677–8692, 2021
https://doi.org/10.5194/acp-21-8677-2021-supplement
© Author(s) 2021. CC BY 4.0 License.

Supplement of

Substantial changes in gaseous pollutants and chemical compositions in fine particles in the North China Plain during the COVID-19 lockdown period: anthropogenic vs. meteorological influences

Rui Li et al.

Correspondence to: Hongbo Fu (fuhb@fudan.edu.cn), Jianmin Chen (jmchen@fudan.edu.cn), and Meng Peng (mvponesky@163.com)

The copyright of individual parts of the supplement might differ from the article licence.

Text S1 Data quality assurance of chemical compositions in $PM_{2.5}$

The NH_3 concentration and water-soluble ions including sulfate (SO_4^{2-}), nitrate (NO_3^-), ammonium (NH_4^+), sodium ion (Na^+), and chloridion (Cl^-) were monitored with a Gas and Aerosol Collector combined with Ion Chromatography (GAC-IC, TH-PKU-303, China). The concentration gradients of anion and cation standard solutions were set based on the pollution levels of target species, and correlation coefficients of the calibration curve were highly correlated, with r^2 of 0.99 and slope closing to 1, indicating good quality of the dataset.

Trace elements in $PM_{2.5}$ were measured using a Xact multi-metal monitor (Model Xact 625, Cooper Environment Service, USA). Ambient $PM_{2.5}$ was collected using a cyclone inlet at a flow rate of 16.7 L min^{-1} and deposited on a filter tape. The mass concentrations of trace elements were determined using X-ray fluorescence (XRF). In each measurement, the detector energy gain was automatically adapted using pure Pd as an internal standard. The XRF response of the interest element was calibrated using the standard thin-film provided by the manufacturer. The measured mass was well in agreement with standard mass for each element and the deviation was less than 5%. The minimum detection limits (ng m^{-3}) of elements for 1-hour collection are shown in Table S1.

OC and EC were measured using an OC/EC analyzer (Model RT-4, Sunset Laboratory Inc., Tigard, Oregon, USA). Briefly, the ambient aerosol was collected with a $PM_{2.5}$ cyclone inlet at a flow rate of 8 L min^{-1} and then deposited on a 16-mm diameter quartz filter punch. In each hour cycle, the sampling time and analysis time were 45-min and 15-min respectively. OC deposited on the filter was firstly volatized into carbon dioxide (CO_2) by a manganese dioxide (MnO_2) catalyst in an oxygen-free atmosphere with helium as a carrier gas. CO_2 levels were quantified by a nondispersive infrared detector. During this stage, a fraction of OC was pyrolyzed into pyrolyzed carbon (PC). In the next stage, EC and PC are combusted in an oxygen atmosphere. All carbon fractions volatized before PC combustion were regarded as OC and those after PC combustion were EC through the thermal-optical transmission protocol. At the end of each analysis, a known amount of methane (5% CH_4 in He) was injected as the internal calibration for quality control.

Figure S1 The performance of the random forest model in predicting the hourly concentrations of gaseous pollutants. The model was constructed with 90% original data and the remained data was applied to validate the model. The black solid line denotes the best-fitting curve for all of the points, while the black dashed line represents the diagonal, which means the same observed and simulated values.

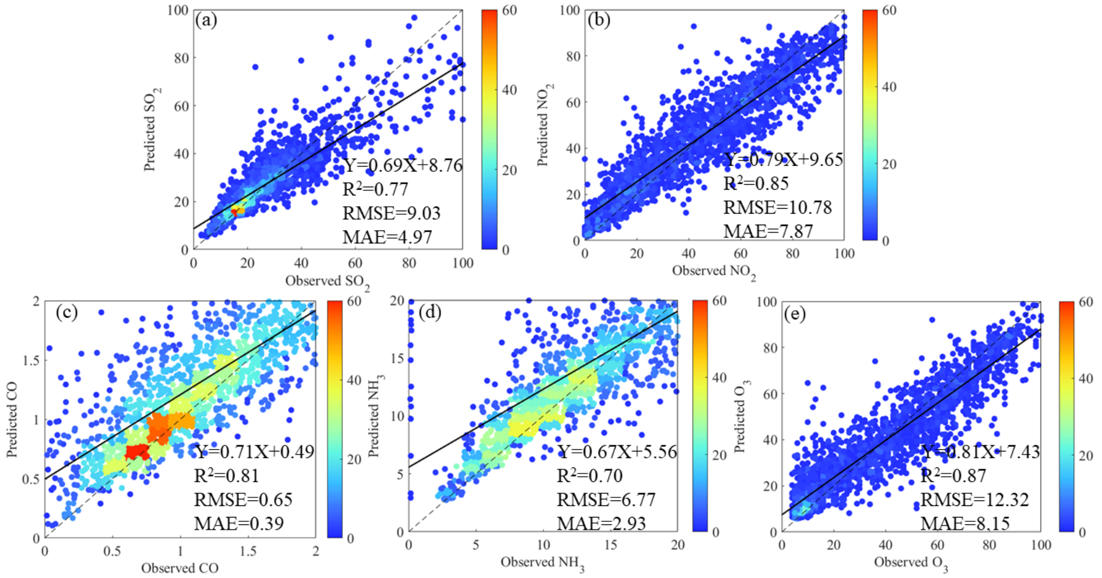

Figure S2 The performance of the random forest model in predicting the hourly concentrations of water-soluble ions in $PM_{2.5}$. The model was constructed with 90% original data and the remained data was applied to validate the model. The black solid line denotes the best-fitting curve for all of the points, while the black dashed line represents the diagonal, which means the same observed and simulated values.

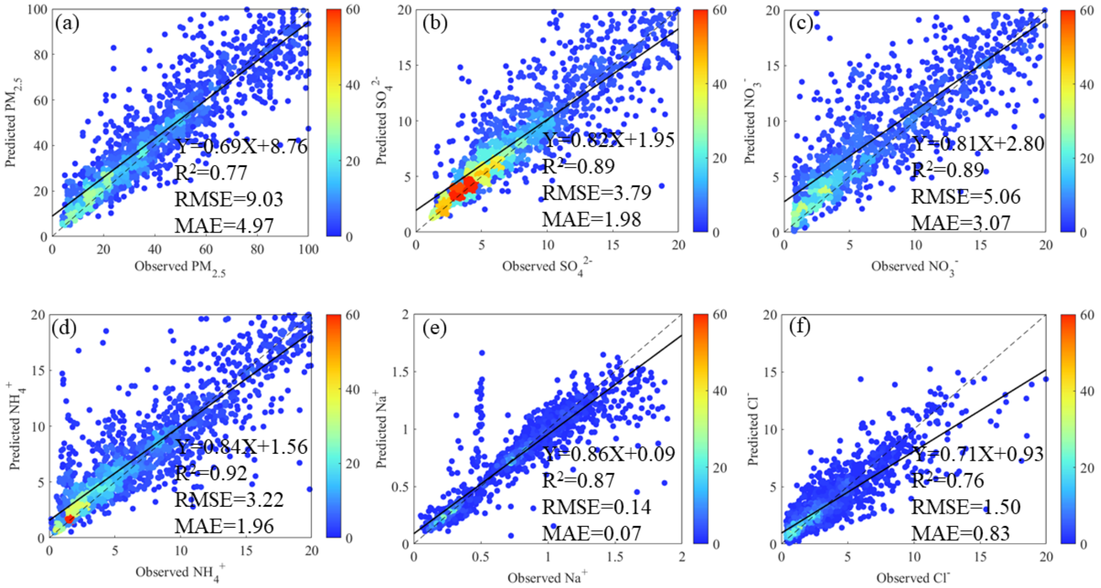

Figure S3 The performance of the random forest model in predicting the hourly concentrations of trace elements in $PM_{2.5}$. The model was constructed with 90% original data and the remained data was applied to validate the model. The black solid line denotes the best-fitting curve for all of the points, while the black dashed line represents the diagonal, which means the same observed and simulated values.

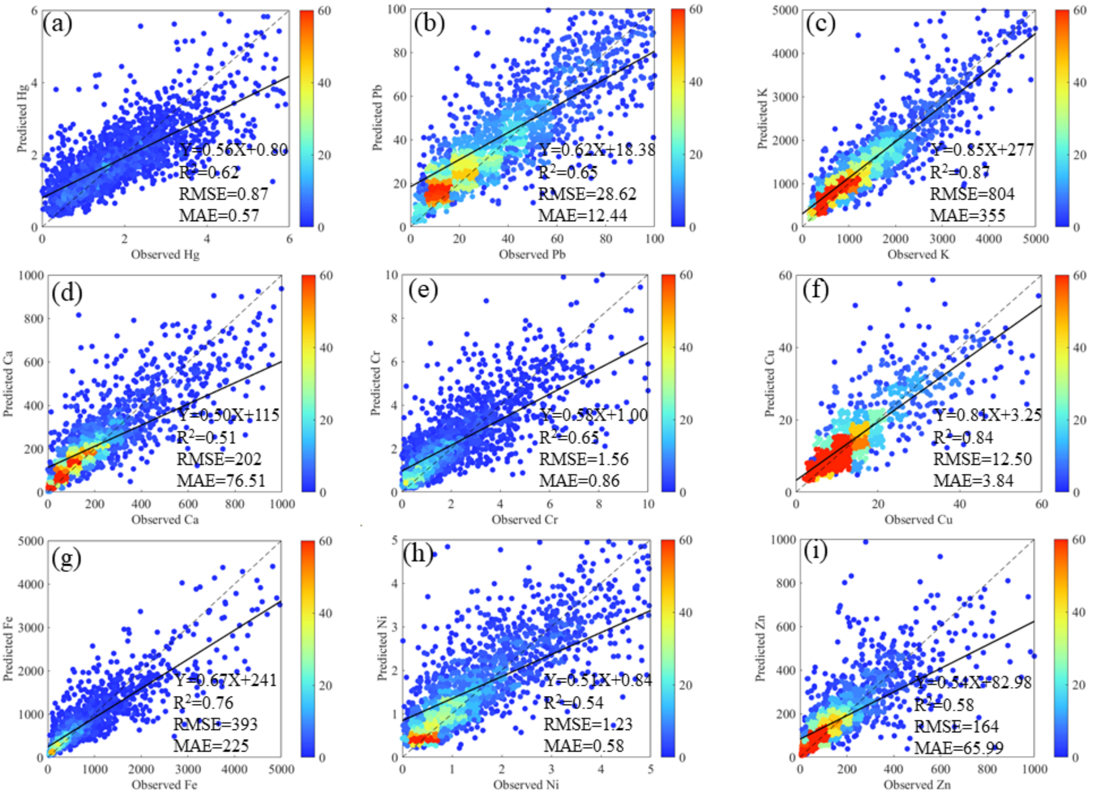

Figure S4 The performance of the random forest model in predicting the hourly concentrations of OC and EC in $PM_{2.5}$. The model was constructed with 90% original data and the remained data was applied to validate the model. The black solid line denotes the best-fitting curve for all of the points, while the black dashed line represents the diagonal, which means the same observed and simulated values.

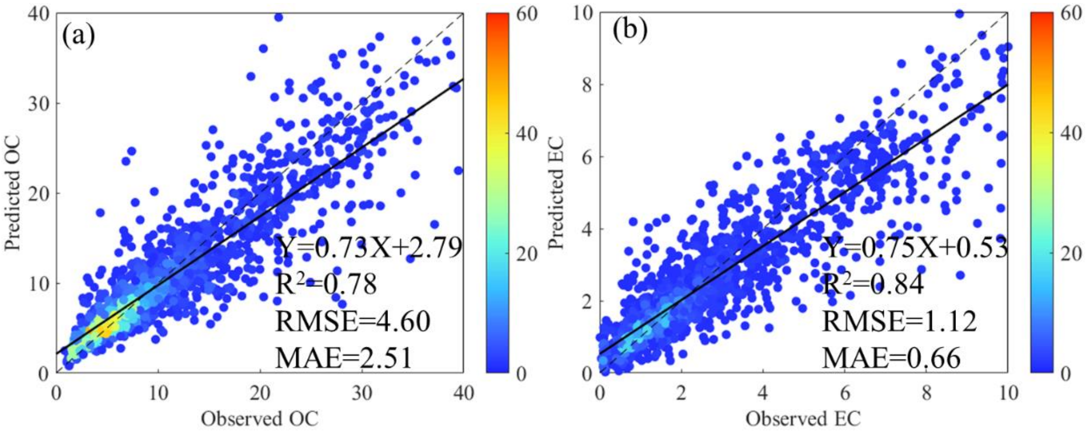

Figure S5 The performance of the random forest model in predicting the hourly concentrations of some other water-soluble ions and trace elements in $PM_{2.5}$. These species generally showed the worse predictive performance and cannot be utilized to distinguish the impacts of meteorology and emission on their temporal variations. The model was constructed with 90% original data and the remained data was applied to validate the model. The black solid line denotes the best-fitting curve for all of the points, while the black dashed line represents the diagonal, which means the same observed and simulated values.

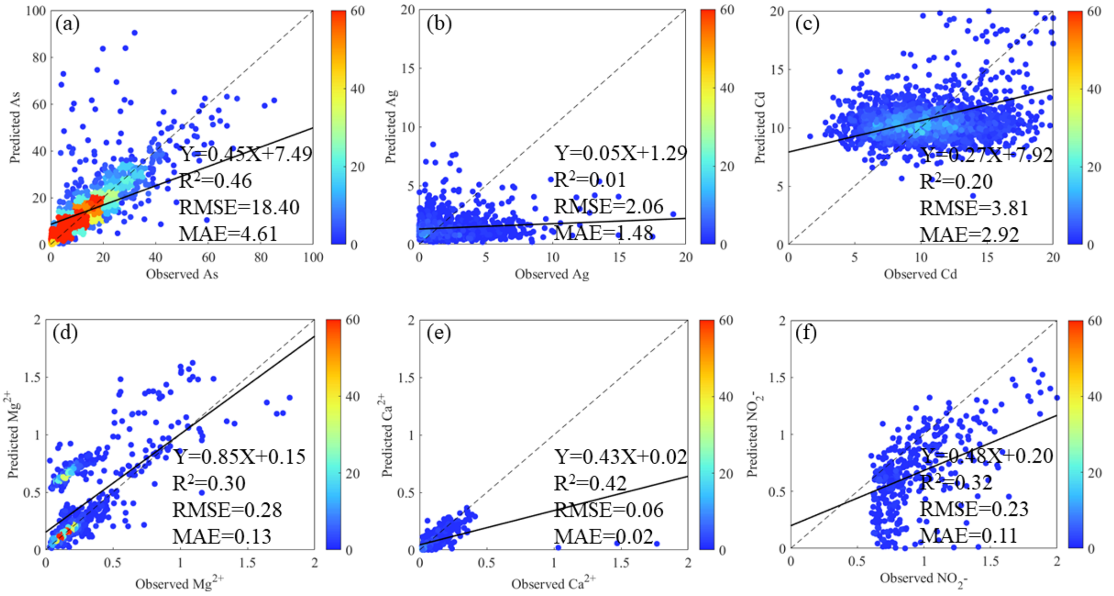

Table S1 The detection limits of the measured chemical species. The units of all of the species except NH_3 were μg/m^3, while the unit of NH_3 is ppb.

Species	IDL
NH_3	0.10
Na^+	0.05
NH_4^+	0.05
Cl^-	0.01
NO_3^-	0.05
SO_4^{2-}	0.05
K	1.17
Ca	0.40
Cr	0.22
Ni	0.15
Fe	0.26
Cu	0.27
Zn	0.23
Hg	0.35
Pb	0.36
OC	0.20
EC	0.20

Table S2 Summary of PMF error diagnostics based on DISP.

Error Code:	0				
The largest decrease in Q:	0				
%dQ	0				
Swaps by Factor:	SF	IP	BB	CC	RD
dQmax=4	0	0	0	0	0
dQmax=8	0	0	0	0	0
dQmax=15	0	0	0	0	0
dQmax=25	0	0	0	0	0

Table S3 Summary of PMF error diagnostics based on BS.

BS Mapping (r≥0.6)	SF	IP	BB	CC	RD	Unmapped
SF	100	0	0	0	0	0
IP	0	100	0	0	0	0
BB	0	0	100	0	0	0
CC	0	2	0	97	1	0
RD	0	0	0	0	100	0

Table S4 Summary of PMF error estimation diagnostics from BS-DISP.

% of Cases Accepted:	97%				
Largest Decrease in Q:	-24.6				
%dQ	-0.0089				
# of Decreases in Q:	1				
# of Swaps in Best Fit:	0				
# of Swaps in DISP:	1				
Swaps by Factor:	SF	IP	BB	CC	RD
dQ^{max}=0.5	0	0	1	0	0
dQ^{max}=1	0	0	1	0	0
dQ^{max}=2	0	0	1	0	0
dQ^{max}=4	0	0	1	0	0